



This is a repository copy of *Evaluation of different particle size distribution and morphology characterization techniques*.

White Rose Research Online URL for this paper:

<https://eprints.whiterose.ac.uk/209940/>

Version: Published Version

Article:

Islam, S.F. orcid.org/0000-0003-1587-7908, Hawkins, S.M., Meyer, J.L.L. et al. (1 more author) (2022) Evaluation of different particle size distribution and morphology characterization techniques. *Additive Manufacturing Letters*, 3. 100077. ISSN 2772-3690

<https://doi.org/10.1016/j.addlet.2022.100077>

Reuse

This article is distributed under the terms of the Creative Commons Attribution (CC BY) licence. This licence allows you to distribute, remix, tweak, and build upon the work, even commercially, as long as you credit the authors for the original work. More information and the full terms of the licence here:

<https://creativecommons.org/licenses/>

Takedown

If you consider content in White Rose Research Online to be in breach of UK law, please notify us by emailing eprints@whiterose.ac.uk including the URL of the record and the reason for the withdrawal request.



eprints@whiterose.ac.uk
<https://eprints.whiterose.ac.uk/>



Evaluation of different particle size distribution and morphology characterization techniques

Syed F. Islam^{a,*}, Scott M. Hawkins^b, John L.L. Meyer^b, Adrian R.C. Sharman^a

^a Advanced Manufacturing Research Centre (AMRC), University of Sheffield, United Kingdom

^b Carpenter Technology Corporation, Reading, PA, United States

ARTICLE INFO

Keywords:

Particle size distribution
Powder characterisation
Morphology
Metal powder
Laser diffraction
Static imaging
Dynamic imaging
Image analysis

ABSTRACT

In this paper, the particle size distribution (PSD) and morphology for six different metal powders were measured and compared using a range of techniques which included laser diffraction, static imaging, and dynamic imaging. The metal powders were chosen from a diverse end-use (Metal Injection Moulding, Laser - Powder Bed Fusion, Electron Beam - Powder Bed Fusion, and Hot Isostatic Pressing) and varied in powder size distribution and morphology. While the results for particles that were predominantly spherical showed some general agreement for the measured PSD across the range of measurement techniques investigated, larger variation than industrial tolerances would allow was identified when comparing the results between the different measurement techniques. The technique did influence the measured PSD at times, with differences large enough to require compensation if used for critical applications with tight tolerances. For samples that had particle morphologies that deviated away from spherical (agglomerated, irregular, or satellited), the difference in the measured PSD was more significant when comparing the results from the different measurement techniques. This was due to the under/overestimation of the PSD due to the measurement principles of the system being employed. Thus, when reporting PSD, it is of paramount importance to align specification requirements, and the certification test methods, with the industrial controls (i.e., laser diffraction when used in production to tune air classification). If different instruments or techniques are to be used by a purchaser and supplier, any inherent bias must be understood. For morphology, static imaging tends to result in a higher measured value for sphericity and aspect ratio in comparison to dynamic imaging. This is believed to be due to the influence of orientation during measurement as well as the resolution of the optics.

1. Introduction

Metal powders are used extensively throughout various industries for numerous applications. The manufacturing method influences the morphology of the produced powder (for example gas atomisation is more spherical in comparison to water atomised powder) [1–3]. The different processes used are dependent on the specification of the powder required (powder size and morphology). The uses of the different specification powders depend on the end product being produced. The particle size distribution (PSD) of the powders varies greatly depending on the application. Certain applications such as additive manufacturing (AM) require powder that is highly spherical for controlled and predictable flowability/spreadability as well as packing density [4]. It is common for the powder to be recycled when used for AM applications, and therefore any changes in the PSD and morphology need to be monitored to ensure the powder remains in specification [5,6]. For example, if the PSD is too fine, spatter formation may increase due to the

excess laser power/energy density, or if the powder PSD becomes too coarse, not all the particles will melt due to insufficient laser power [7,8]. These bring about different defects and may ultimately result in a part with reduced properties or a failed build. Work conducted concerning Laser-Powder Bed Fusion (L-PBF) recycling has shown that continual recycling of powder increases the mean PSD and decreases the circularity (2D information), which ultimately affected the quality of the fabricated part [5]. Furthermore, certain powder materials (e.g. aluminium based) are more sensitive to reuse in terms of the change in PSD and morphology which makes monitoring the reuse of powder important [9].

The desire is to have a consistent powder in terms of PSD and morphology for reliable flowability (other factors also influence flowability e.g. moisture and temperature). The correct powder characterisation allows the appropriate quality control to be in place to ensure that powder behaviour is predictable and repeatable across different batches. A variable powder supply will ultimately affect product quality and lead to

* Corresponding author at: The University of Sheffield AMRC: The University of Sheffield Advanced Manufacturing Research Centre, United Kingdom
E-mail address: s.f.islam@sheffield.ac.uk (S.F. Islam).

variations that are unacceptable for certain industries such as medical and aerospace [10].

There are several methods available to characterise the size and morphology of powder. Dependent on the method used, the results will vary in terms of the measured PSD. Thus, an understanding and appreciation of the method used, and its assumptions when calculating the PSD or morphology data is of importance [11]. Sieving is one of the oldest and most established techniques, with its principle based on a series of sieve aperture dimensions stacked progressively. This sorting by two-dimensional opening can result in particles with irregular morphologies, such as elongated, passing through (if the orientation is such that the smallest cross-section can pass through the mesh opening). This technique is ideal for specifying and certifying any powder sorted in production through a sieving process. For gas-atomized powder, sieving is typically performed in production down to 45 μm , below which agglomerated powder can 'blind' the sieves. The sieving test method can be labour and time-intensive and only provides limited size discrimination. The large test sample offers high sampling statistics, and the mechanism is aligned with the two-dimensional sorting mechanism in production, limiting discrepancies between the production control (industrial sieve cloth) and the quality control (certifying sieves).

Laser diffraction is a faster and automated technique based on measuring the angle of diffraction, reflection, and refraction of the laser as a sample passes through it, as these angles are proportional to its size. The scattering of the laser is recorded by detectors situated within the machine which then process the pattern to calculate the equivalent spherical diameter as calibrated by perfectly spherical glass beads. Therefore, laser diffraction is influenced by particle morphology as anything other than perfectly spherical will result in a different diffraction angle dependent on the orientation of the sample as it passes through the laser beam(s) path [12]. The measurement may take place in air (dry) or a liquid (wet) medium. The need for a wet measurement may be necessary if the sample being measured is flammable or for cohesive powder. In the analysis, light scattering data is converted, via proprietary algorithms specific to the instrument manufacturer, into volumetric particle size distribution. Although this technique only requires a small sample size, sampling errors due to non-standard distributions or morphology effects can be exacerbated, especially at the tails of the distribution (high and low length/width aspect ratios).

Imaging is another commonly used approach, for particle size measurement [13]. It involves capturing and processing thousands of images of particles. It is easier to ensure static images are in focus as the field of focus is fixed, whereas for a dynamic image this can become an issue as the sample may move into or out of focus during measurement. Imaging offers an additional advantage over sieving and laser techniques in that it offers information not only relating to size but also the morphology of the particles (2D information). This is important as the manufacturing processes of metal powders vary drastically and the powder can range from perfectly spherical, elongated, to agglomerate, to irregular, to satellited. Furthermore, this becomes important for example when recycling powder, as subtle changes may occur that slightly change the morphology of the powder (without changing the PSD significantly) [14]. Work has been conducted comparing 2D measurement techniques (imaging) with 3D (X-ray CT), which has discrepancies and requires significant time for measurements. Further work is being conducted in this area to better understand how better use can be made of the 2D measurement technique [15].

The PSD of powder is often reported in percentiles: D_{10} , D_{50} and D_{90} . The D_{10} refers to the diameter size below which 10% of the powder by mass or volume is finer than, D_{50} refers to the mean diameter size for which 50% of the sample mass or volume is finer than, and D_{90} refers to the diameter size which 10% of the powder by mass or volume is coarser than. The size distribution can be presented in various forms, ranging from the number basis where the fines would dominate the PSD, to a volume or mass basis where the larger particles are more influential. If the powder being measured is homogenous and of the same density,

the mass fraction can be converted to volume fraction and vice versa [16,17].

At present, there is limited work to show the effect of different powder characterisation techniques in terms of measured particle size distribution and morphology for metal powders with a range of sizes. Research has been conducted on Aluminium and Tantalum powders showing the carrier fluid speed and ultrasonic power had no substantial effect on the measured PSD using laser diffraction [18]. Further research looking at X-ray CT and SEM as measurement techniques for analysing steel powders showed these to be more robust than commonly used techniques, though they are time-consuming and not appropriate for quality control purposes [19]. The current work compares imaging (dynamic and static) and laser diffraction (wet and dry) techniques for metal powders with a variety of particle size distributions to understand how PSD and morphology results vary due to measurement technique and instrument-to-instrument differences.

2. Materials and methods

2.1. Samples

Six metal powders for various industrial applications were studied (supplied by Carpenter Technology Corporation). The powder was selected to intentionally vary size, morphology, satelliting, and agglomeration. All powders were manufactured via gas atomisation and are as follows:

- Powder 1 - Carpenter Technology UltraFine® 316L used for Metal Injection Moulding (MIM), which was air classified to $D_{90} < 22 \mu\text{m}$
- Powder 2 - Carpenter Additive® M300 used for L-PBF, which was screened with a vibratory screener with a wire mesh at 45 μm for the top end and air classified at 15 μm at the bottom end
- Powder 3 - Carpenter Additive® XLC used for L-PBF, which was screened with a vibratory screener with a wire mesh at 45 μm for the top end and air classified at 15 μm at the bottom end
- Powder 4 - Carpenter Additive® Ti64 Gd5 used for Electron Beam – Powder Bed Fusion (EB-PBF), which was screened with a vibratory screener with a wire mesh at 106 μm for the top end and 45 μm at the bottom end
- Powder 5 - Carpenter Technology Micro-Melt® 625 used for Hot Isostatic Pressing (HIP), which was screened with a vibratory screener with a wire mesh at 250 μm for the top end and no screening at the bottom end
- Powder 6 - Carpenter Technology Micro-Melt® BioDur® CCM® used for HIP, which was screened with a vibratory screener with a wire mesh at 250 μm for the top end and no screening at the bottom end.

2.2. Powder analysis methods

2.2.1. Particle size distribution

The PSD was measured using two different laser diffraction systems, a Mastersizer 3000 (Malvern, UK), for both dry and wet measurements (Aero S and Hydro EV, referred to as LD-D and LD-W1 respectively throughout the paper), and the Microtrac S3500 for wet measurements (Microtrac, USA, referred to as LD-W2 throughout the paper). Wet measurements were conducted in water at room temperature. There is a range of different scattering theories used for particle size analysis, with the main ones being Mie and Fraunhofer (details on the different theories are outside the scope of this paper) [16]. The Mie theory was applied for the analysis of the data scattering pattern using the relevant refractive indices provided by the manufacturer for the materials being measured.

The PSD was further measured using the dynamic imaging (DI) technique on a Camsizer XT (Microtrac, UK) using a dry dispersion jet with a dispersion pressure of 40 kPa. Also, the PSD was measured using the

Table 1

Comparison of the different sample quantities required and duration for conducting a measurement on the different test methods (*general limit for acceptable sieving as opposed to resolution limit).

Equipment	No. of particles	Time (min.)	Mass (g)	Resolution Limit (μm)	Data output
Static imaging	$\approx 10^4 - 10^5$	≈ 120	$\approx 0.01 - 0.03$	0.50	PSD & Morphology
Laser diffraction	$\approx 10^5 - 10^6$	≈ 10	≈ 2.0	0.01/0.02	PSD
Dynamic imaging	$\approx 10^6 - 10^8$	≈ 10	≈ 10.0	1	PSD & Morphology
Sieve analysis	$\approx 10^7 - 10^9$	≈ 15	50 or 100	< 45*	PSD

static imaging (SI) technique on a Morphologi G3SE (Malvern, UK) using a dispersion pressure of 400 kPa. The PSD data for both imaging techniques were populated based on the area principle, which converts the measured area of a particle into the equivalent diameter of a circle.

The static imaging system takes images of the powder sample after it is spread on a glass slide (which is cleaned before using Sticklers spray which dissipates static forces and lens cleaning tissue). The powder is spread and allowed to settle under gravity. The powder takes the orientation which is most stable for it when settling on the glass slide. Furthermore, the sample quantity measured is significantly less for the SI in comparison to the other techniques (Table 1), which makes it possible that if a few of the larger particles are missed during sample selection, it can result in an underestimation of the PSD drastically.

The dynamic imaging technique takes images as the powder sample travels past the camera. Therefore, images are taken of the sample during various orientations of the powder, and not solely one orientation. Thus, the DI is less influenced by the orientation of the sample (though particles will sometimes align because of the airflow while falling) and produces results similar to the LD systems. Furthermore, the sample quantity measured in the DI is significantly higher in comparison to the other techniques (Table 1) and the probability of missing some of the larger particles during sample selection is minimised.

All PSD measurements were conducted on a volume basis. For the laser diffraction and dynamic imaging systems, three measurements were conducted on each powder sample. For the static imaging system, one measurement was conducted on each powder sample (due to the time required for measurement per sample).

2.2.2. Morphology

Morphology measurements were conducted on the Camsizer XT and Morphologi G3SE. The morphology was characterised in terms of sphericity and aspect ratio. The sphericity is a measure of how closely the shape of the particle(s) sampled is compared to that of a perfect circle. A perfect sphere or circular cross-section would have a sphericity of 1, while a needle-like morphology would have a sphericity value closer to zero. The Camsizer XT uses the term 'Sphericity' while the Morphologi G3 uses the term 'High Sensitivity Circularity'. They are calculated using the same equation, though they are referred to differently. The equation to calculate the sphericity is as follows:

$$\begin{aligned} \text{Sphericity (Camsizer XT)} &= \frac{4\pi \text{Area}}{\text{Perimeter}^2} \\ &= \text{High Sensitivity Circularity (Morphologi G3)} \end{aligned}$$

Where the Area is the measured particle area and Perimeter is the measured particle perimeter.

The aspect ratio is the ratio of the minimum chord length ($X_{c, \min}$ or width) to the maximum Feret diameter ($X_{Fe, \max}$ or breadth or length) of a particle. The Camsizer XT uses the term 'b/l' while the Morphologi G3 uses the term 'Aspect Ratio'. A circle or square would have an aspect ratio of 1, while a needle-like or rectangular particle morphology would have an aspect ratio lower than 1. The equation to calculate the aspect ratio is as follows:

$$\begin{aligned} b/l \text{ (Camsizer XT)} &= \frac{X_{c, \min}}{X_{Fe, \max}} = \frac{\text{Breadth}}{\text{Length}} = \frac{\text{Width}}{\text{Length}} \\ &= \text{Aspect Ratio (Morphologi G3)} \end{aligned}$$

Where Length is greater than Width.

Additionally, images of the powder were taken using a scanning electron microscope (SEM, Carl Zeiss Evo LS25) using a backscatter electron detector, with a beam landing energy of 20.00 kV and beam current of 10.0 nA for all samples. A powder sample was spread onto a carbon tab adhered to a specimen stub.

2.3. Equipment comparison

The different measurement techniques require a different quantity of samples and duration for the measurement. A comparison of this can be seen in Table 1, with the time quoted referring to a typical measurement time after correct tuning of the operating conditions of the machine. The different quantity of samples required influences the number of particles measured and gives an insight into the potential influence of the results. The static imaging technique requires the longest duration for measuring a sample as high-resolution images are taken of all particles. This time can be reduced if a smaller area of particles is measured, or a Z-stack is not conducted though this will reduce the number of particles analysed and the accuracy of the measurement. The dynamic imaging technique also offers morphological information, in addition to PSD data, however, it does not store all the images taken of the sample during the measurements. The laser diffraction and sieving system only provide PSD data.

The approximate number of particles measured quoted in Table 1 is calculated based on the mass of the sample required for the measurement technique and using the particle count information provided by the static imaging and dynamic imaging techniques. The resolution limit refers to the smallest measurable particles for the system (sieving resolution limit refers to the general limit for acceptable sieving).

For the laser diffraction and dynamic imaging techniques, three measurements were conducted with the mean presented. For the static imaging technique, one measurement for each sample was conducted.

3. Results and Discussion

3.1. SEM images

An SEM micrograph for Powder 1 can be seen in Fig. 1. It can be seen in the SEM image that predominantly the particles appear generally spherical, however, some particles exhibit irregular morphology. There is also a large presence of fines which is expected for this powder, as it has a $D_{90} < 22 \mu\text{m}$.

SEM micrographs for Powder 2 and Powder 3 can be seen in Fig. 2 and Fig. 3, respectively. There is the presence of agglomerates (red arrow) and satellites (yellow arrow) as well as some spherical particles. It can be seen from the micrograph that the agglomerate is composed of many fine particles. The surface of the particles appears generally smooth.

SEM micrographs for Powder 4 can be seen in Fig. 4. It can be seen in the image that the powder is predominantly spherical, though there is a presence of small satellites which are adhered to the surface of the powder.

SEM micrographs for Powder 5 and Powder 6 can be seen in Fig. 5 and Fig. 6, respectively. The surface of Powder 5 appears smoother in comparison to Powder 6. Satelliting and agglomeration are amplified

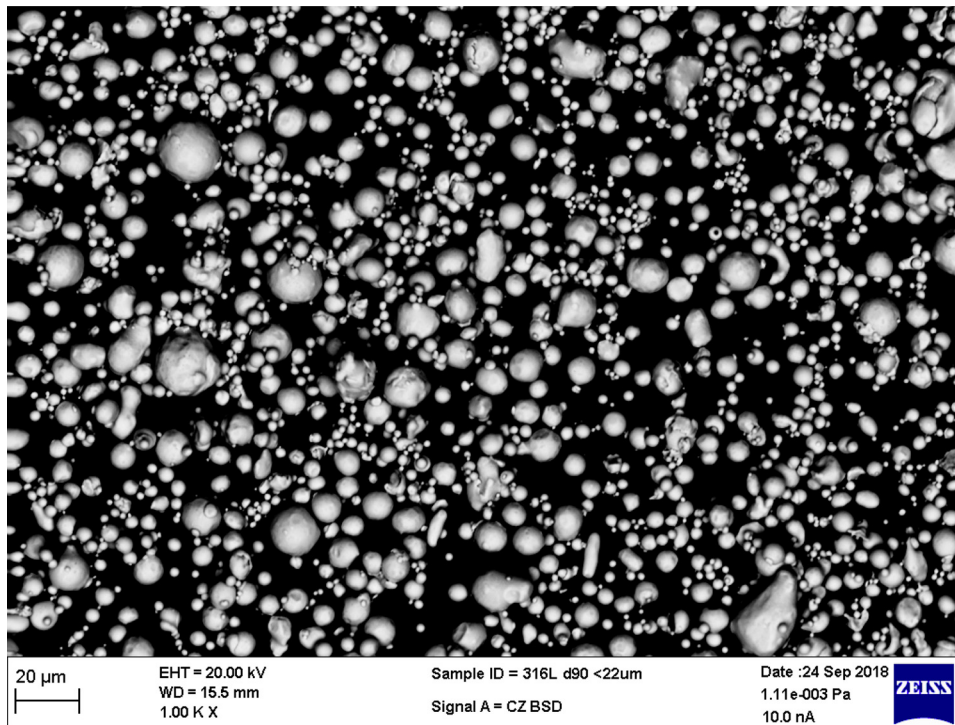


Fig. 1. SEM micrograph for Powder 1, MIM, $D_{90} < 22 \mu\text{m}$ (1000 x magnification).

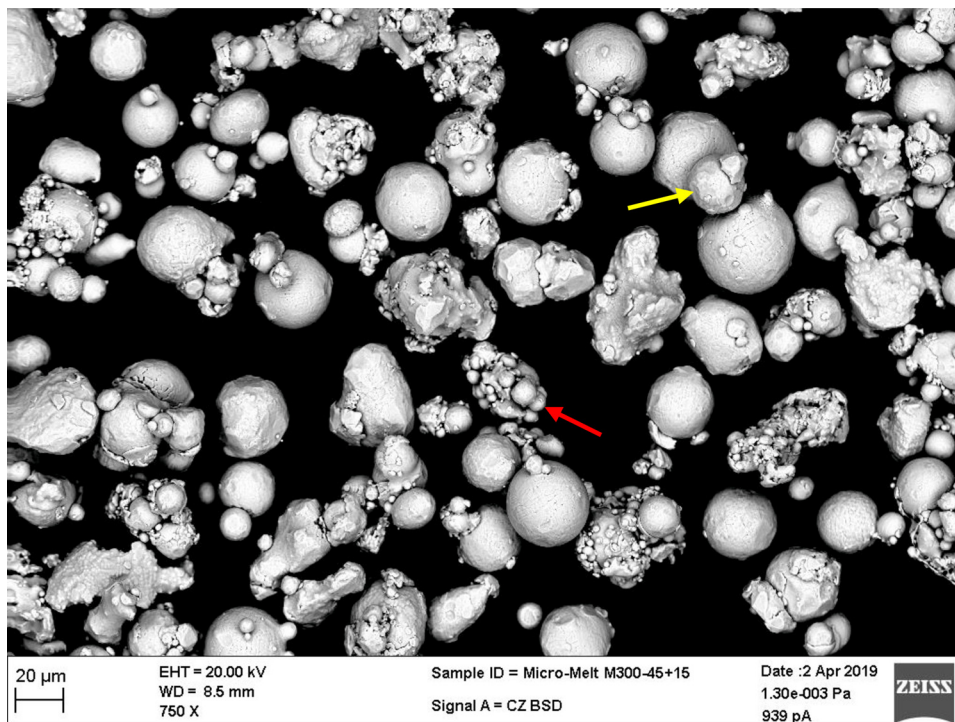


Fig. 2. SEM micrograph for Powder 2, L-PBF, 15 - 45 μm (750 x magnification).

for the HIP powders in comparison to the L-PBF and EB-PBF powders. The smaller surface-bearing particles are a combination of smaller particles fused on the surface of larger particles (satellites, yellow arrow) and, separately, smaller particles that are loosely adhered to the surface of larger particles (agglomerates, red arrow). The presence of satellites is common for powder manufactured via conventional gas atomisation. The formation of satellites occurs during the solidification stage of atomisation, as molten material adheres to partially- or fully-solidified material as the particles collide with one another [20].

3.2. PSD data

The PSD for Powder 1 (MIM) can be seen in Table 2. There is poor (D_{10} spread of $\pm 13\%$, D_{50} spread of $\pm 10\%$, D_{90} spread of $\pm 4\%$) agreement across the different measurement techniques, with the greatest difference in values seen for the D_{50} of 2.9 μm between the DI and the LD-W1. The powder is specified to have a $D_{90} < 22 \mu\text{m}$, and it can be seen from Table 2 that all measurement techniques fall close to this but the spread in the results between techniques/instruments is unacceptable

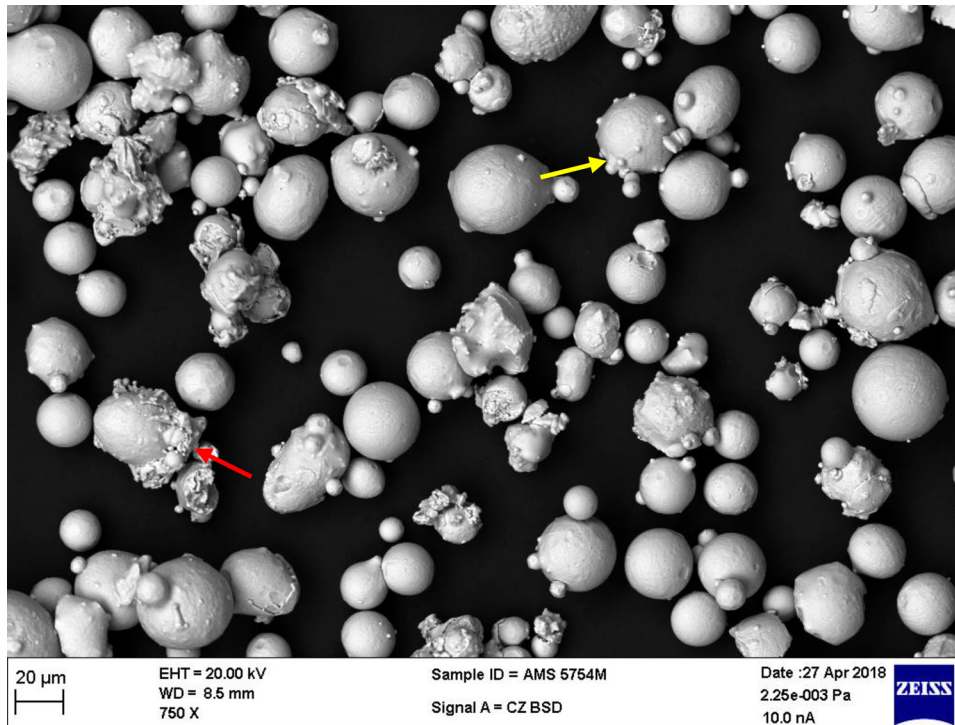
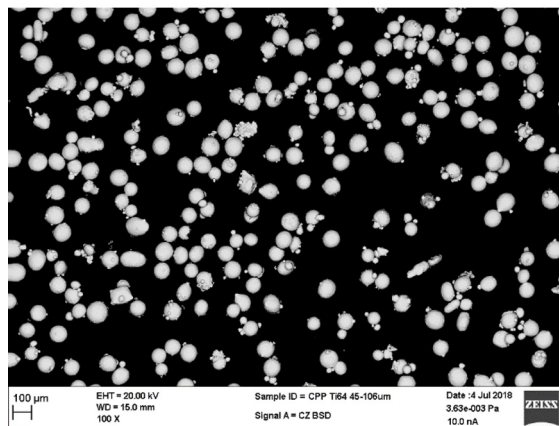
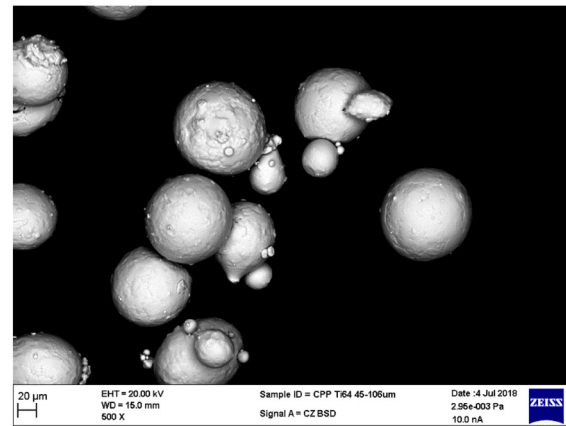


Fig. 3. SEM micrograph for Powder 3, L-PBF, 15 - 45 μm (750 x magnification).



100 x



500 x

Fig. 4. SEM micrographs for Powder 4, EB-PBF, 45 - 106 μm .

in comparison to the manufacturers' internal tolerance and customer requirements ($D_{90} < 22 \mu\text{m}$)

The PSD data for Powder 2 and Powder 3 (L-PBF) can be seen in Table 3. There is some ($\pm 3\text{-}4\%$) agreement across the different measurement techniques for the D_{50} . For the D_{10} , there is good ($\pm 1\%$) agreement between the optical methods (DI and SI) but poorer ($\pm 6\text{-}8\%$) agreement for the laser methods (LD-D, LD-W1 and LD-W2). For the D_{90} , there is a good agreement when comparing the different laser techniques (LD-D, LD-W1 and LD-W2) with each other ($\pm 1\text{-}3\%$) and the optical imaging techniques (DI and SI) with each other ($\pm 0.2\text{-}0.6\%$), however, there is a large difference when comparing the laser and imaging techniques. The laser techniques measure approximately 50 μm for the D_{90} for both L-PBF powders, whereas for the imaging the D_{90} measures closer to 46 μm . One of the reasons believed for this large difference in the D_{90} is the satellites that are attached to some of the larger particles and the presence of agglomerates (Fig. 2 & Fig. 3). This is known to influence

measurement results greatly via laser diffraction as the particles deviate away from spherical [21]. These particles of satellited/irregular morphology may influence the diffraction angles when passing through the path of the laser beam depending on the orientation, thus, resulting in overestimates of the size. Furthermore, for the imaging technique, some of these satellites may be missed during measurement, as any satellites positioned either behind or in front of the particle will not be taken into consideration for the measurement as it only considers the boundaries of the silhouettes. Additionally, these results underscore the importance of aligning specification and certification methods to production controls as the $D_{99,9}$ by sieve analysis is $\approx 45 \mu\text{m}$. Although laser and optical methods provide consistent results, both 1D simplifications overestimate the 2D sorting of sieve by a significant margin. To create specifications using laser or optical results one must establish the bias between the industrial production controls (sieving) and the desired inspection instrument (laser or optical).

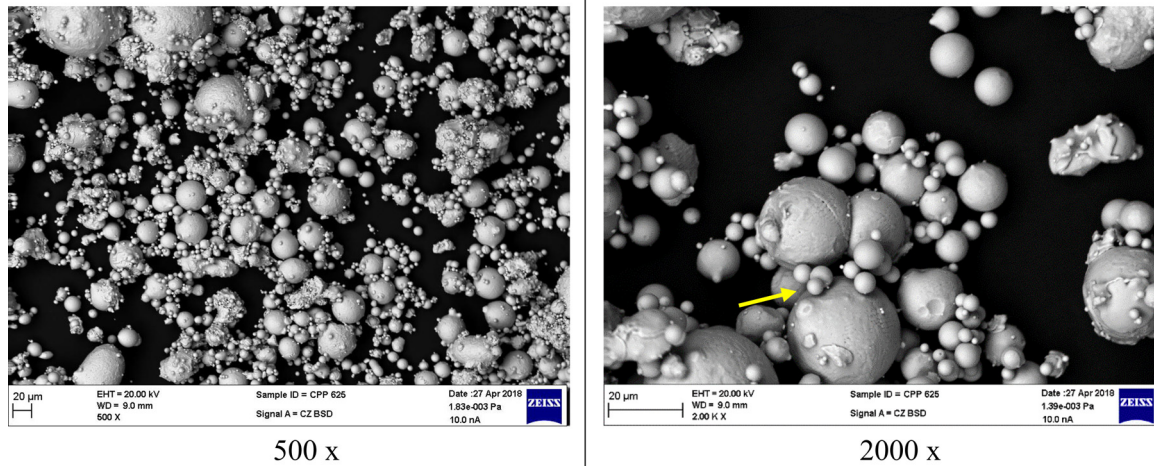


Fig. 5. SEM micrographs at different magnifications for Powder 5, HIP, sieved using 250 µm mesh.

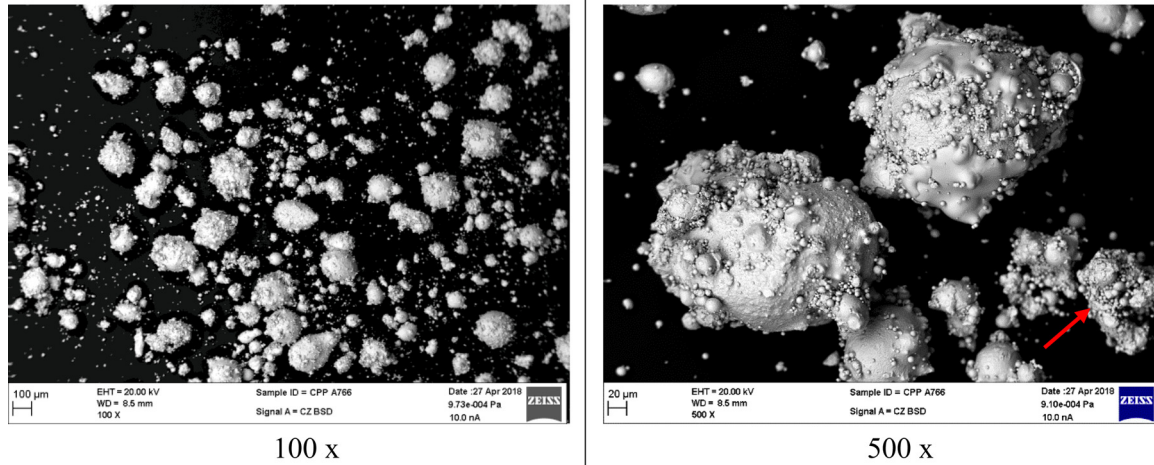


Fig. 6. SEM micrographs at different magnifications for Powder 6, HIP, sieved using 250 µm mesh.

Table 2

Measured PSD data for Powder 1, MIM (The mean values are presented along with the calculated standard deviations).

		D ₁₀ (µm)	D ₅₀ (µm)	D ₉₀ (µm)
LD-D		5.97 (±0.02)	13.70 (±0.01)	24.09 (±0.01)
LD-W1		5.92 (±0.06)	12.96 (±0.11)	23.57 (±0.15)
LD-W2		6.74 (±0.12)	14.28 (±0.10)	22.90 (±0.22)
DI		7.63 (±0.06)	15.87 (±0.06)	24.13 (±0.15)
SI		6.36	13.60	22.22
Mean	All	6.5	14.1	23.4
	Laser	6.2	13.6	23.5
	Optical	7.0	14.7	23.2
Spread (Max.–Min.)/2	All	±13%	±10%	±4%
	Laser	±7%	±5%	±3%
	Optical	±9%	±8%	±4%

The PSD data for Powder 4 (EB-PBF) can be seen in Table 4. There is a wider variance between the different equipment for the D₁₀, D₅₀, and D₉₀ in comparison to the L-PBF powders (Table 3). The largest difference of 19.9 µm is seen for the D₅₀ value, between the SI and LD-W2. This is believed to be due to the dispersion method of the Morphologi and the low density of Powder 4 resulting in less fine powder being transferred to

the imaging slide. The loss of a small portion of fine particles, coupled with the small initial sample size used in the SI technique may have significantly altered this result.

The PSD data for Powder 5 and Powder 6 (HIP) can be seen in Table 5, along with the graphs of the data in Fig. 7 and Fig. 8, respectively. There is a wide variance between the D₅₀, and even more so for the D₉₀, in comparison to the MIM, L-PBF, and EB-PBF powders (Powders 1 – 4). The largest difference of 101.3 µm is seen for the D₉₀ value for Powder 6 between the SI and LD-D. A similar large difference is seen for the D₉₀ value of Powder 5 of 70.5 µm, again between the SI and LD-D. This is believed to be due to preferential dispersion of fine powder and small sample size resulting in relatively fewer coarse particles landing on the imaging stage. The morphology of some of the larger particles may cause additional discrepancies. The SEM images for both HIP powders (Fig. 5 & Fig. 6), show the presence of agglomerates and satellites on some of the larger particles.

The HIP powders, seem to be emphasised with the LD-D system (DI as well for the D₉₀ values for both Powder 5 and 6), which may be measuring the particles agglomerated together as opposed to individually as they pass the beam path. Thus, overestimating the PSD of the sample drastically, which may be the case for the results seen. This is not an issue for the wet systems, as the liquid medium disperses the sample ap-

Table 3

Measured PSD data for Powder 2 and Powder 3, L-PBF (The mean values are presented along with the calculated standard deviations).

		Powder 2				Powder 3			
		D ₁₀ (µm)	D ₅₀ (µm)	D ₉₀ (µm)	D _{99,9} (µm)	D ₁₀ (µm)	D ₅₀ (µm)	D ₉₀ (µm)	D _{99,9} (µm)
LD-D		24.30 (±0.10)	34.63 (±0.06)	49.40 (±0.20)		21.19 (±0.01)	32.23 (±0.06)	49.10 (±0.10)	
LD-W1		22.93 (±0.12)	33.77 (±0.12)	49.37 (±0.25)		19.73 (±0.15)	31.23 (±0.15)	49.20 (±0.10)	
LD-W2		25.72 (±0.44)	35.61 (±0.60)	51.90 (±1.47)		23.10 (±0.80)	33.53 (±0.46)	50.04 (±1.12)	
DI		26.13 (±0.12)	36.10 (±0.17)	45.53 (±0.06)		22.97 (±0.06)	33.43 (±0.12)	45.70 (±0.30)	
SI		25.66	36.21	45.67		22.36	33.85	46.29	
Sieve					45				45
Mean	All	24.95	35.27	48.38		21.87	32.86	48.07	
	Laser	24.32	34.67	50.20		21.34	32.33	49.40	
	Optical	25.90	36.16	45.60		22.66	33.64	46.00	
Spread	All	±6%	±3%	±7%		±8%	±4%	±5%	
(Max.–Min.)/2	Laser	±6%	±3%	±3%		±8%	±4%	±1%	
Mean	Optical	±0.9%	±0.2%	±0.2%		±1.3%	±0.6%	±0.6%	

Table 4

Measured PSD data for Powder 4, EB-PBF (The mean values are presented along with the calculated standard deviations).

		D ₁₀ (µm)	D ₅₀ (µm)	D ₉₀ (µm)
LD-D		54.23 (±2.41)	75.80 (±3.87)	106.0 (±5.29)
LD-W1		49.20 (±0.46)	74.53 (±0.06)	110.3 (±0.58)
LD-W2		50.72 (±2.11)	70.41 (±2.42)	105.6 (±2.94)
DI		52.40 (±1.06)	76.40 (±3.14)	103.8 (±2.00)
SI		64.92	90.3	107.4
Mean	All	54.30	77.49	106.63
	Laser	51.39	73.58	107.32
	Optical	58.66	83.35	105.60
Spread	All	±14%	±13%	±3%
(Max.–Min.)/2	Laser	±5%	±4%	±2%
Mean	Optical	±11%	±8%	±2%

appropriately and helps to reduce the potential for agglomeration of fines during the measurement.

In addition to some of the reasons mentioned already, it should also be noted for the wet dispersion systems, the samples are circulated continuously during measurements meaning that there is the potential for certain particles to be measured multiple times depending on the speed at which they travel. Furthermore, the impeller which is driving the sample may break up some of the agglomerates/satellites if they come into direct contact. As well as this, some of the larger/heavier particles may settle on the bottom or within the tubing system (build-up of powder in the tubing was seen in between some measurements). For the dry dispersion system, the sample only passes via the optics once for measurement and it is possible during the measurement that weakly bonded agglomerates/satellites may be dislodged due to the vibration

of the feeding system, or the application of air pressure to disperse the sample.

3.3. Morphology data

For the morphology analysis, the data from the SI was filtered to remove particles with an area less than 100 pixels (filter not applied for the PSD analysis). This was based on the recommendation of the manufacturer, as small particles are difficult to clearly distinguish based on the resolution, and therefore for morphological analysis, the fine particles should be removed. This removal of particles based on area equated to removing particles smaller than 3.15 µm (in diameter) for Powder 1 and 6.25 µm (in diameter) for Powders 2 – 6 (Optics used for Powder 1 was x10 and for Powders 2 – 6 was x5 based on D₉₀ of powders and recommendations of the manufacturer). For Powders 1 – 4, this resulted in the removal of ≈ 10 to 40 % of particles while for Powders 5 & 6, this resulted in the removal of ≈ 60 % particles (on a number basis). For the DI data, no filters were applied.

The results for the mean sphericity and aspect ratio calculated using both the DI and SI can be seen in Table 6. For all the samples measured, the SI recorded higher sphericity, indicating that the sample was more spherical in comparison to the DI. The highest mean sphericity for the DI from the 6 powders studied was for Powder 4 which, based on the SEM images (Fig. 4), showed the smoothest surface and minimal presence of satellites and agglomerates. For the SI system, the highest mean sphericity was for Powder 1 and Powder 5. For all the samples measured, the SI recorded a higher aspect ratio in comparison to the DI. When comparing the techniques there is general agreement across the range of powders in terms of the highest and lowest values.

Table 5

Measured PSD data for Powder 5 and Powder 6, HIP (The mean values are presented along with the calculated standard deviations).

		Powder 5			Powder 6		
		D ₁₀ (µm)	D ₅₀ (µm)	D ₉₀ (µm)	D ₁₀ (µm)	D ₅₀ (µm)	D ₉₀ (µm)
LD-D		14.73 (±0.29)	53.47 (±0.68)	147.0 (±1.73)	15.33 (±0.21)	59.5 (±1.04)	181.3 (±2.08)
LD-W1		11.47 (±0.23)	37.73 (±0.68)	110.0 (±2.65)	4.82 (±0.32)	32.7 (±0.53)	108.3 (±1.15)
LD-W2		13.48 (±0.21)	42.33 (±1.34)	100.1 (±0.86)	12.57 (±0.20)	38.25 (±2.94)	96.34 (±11.4)
DI		13.43 (±0.21)	40.47 (±1.55)	115.6 (±2.71)	13.57 (±0.15)	39.23 (±0.71)	137.8 (±0.45)
SI		9.30	28.58	76.45	9.75	27.75	79.99
Mean	All	12.48	40.52	109.83	11.21	39.49	120.77
	Laser	13.23	44.51	119.04	10.91	43.48	128.67
	Optical	11.37	34.52	96.03	11.66	33.49	108.91
Spread	All	±22%	±31%	±32%	±47%	±40%	±42%
(Max.–Min.)/2	Laser	±12%	±18%	±20%	±48%	±31%	±33%
Mean	Optical	±18%	±17%	±20%	±16%	±17%	±27%

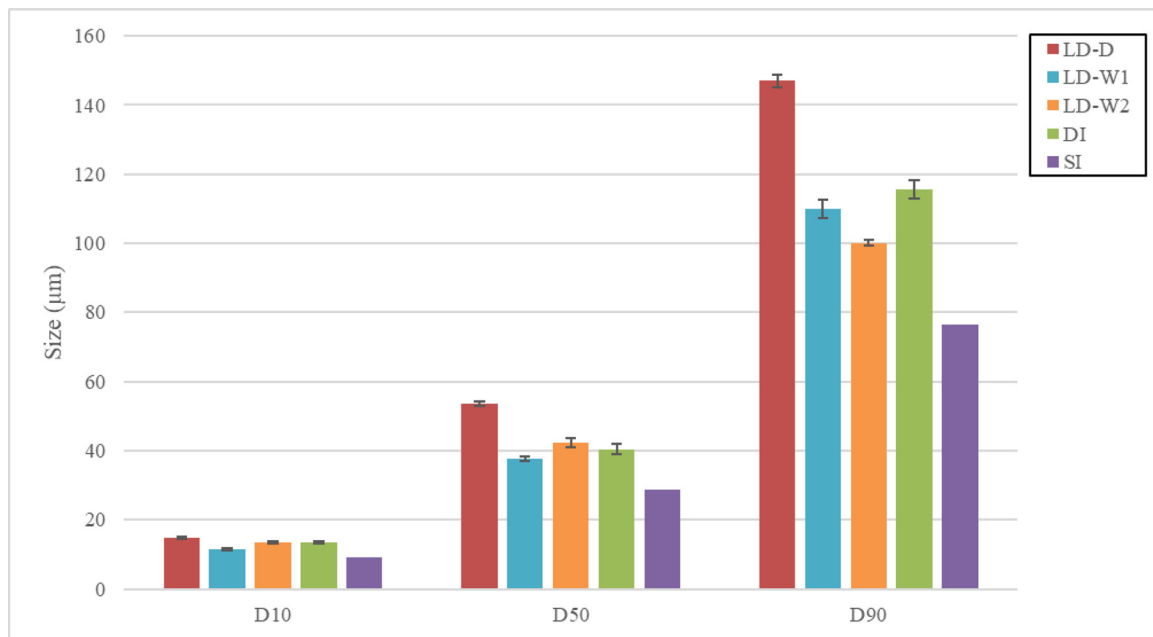


Fig. 7. PSD data for Powder 5, HIP.

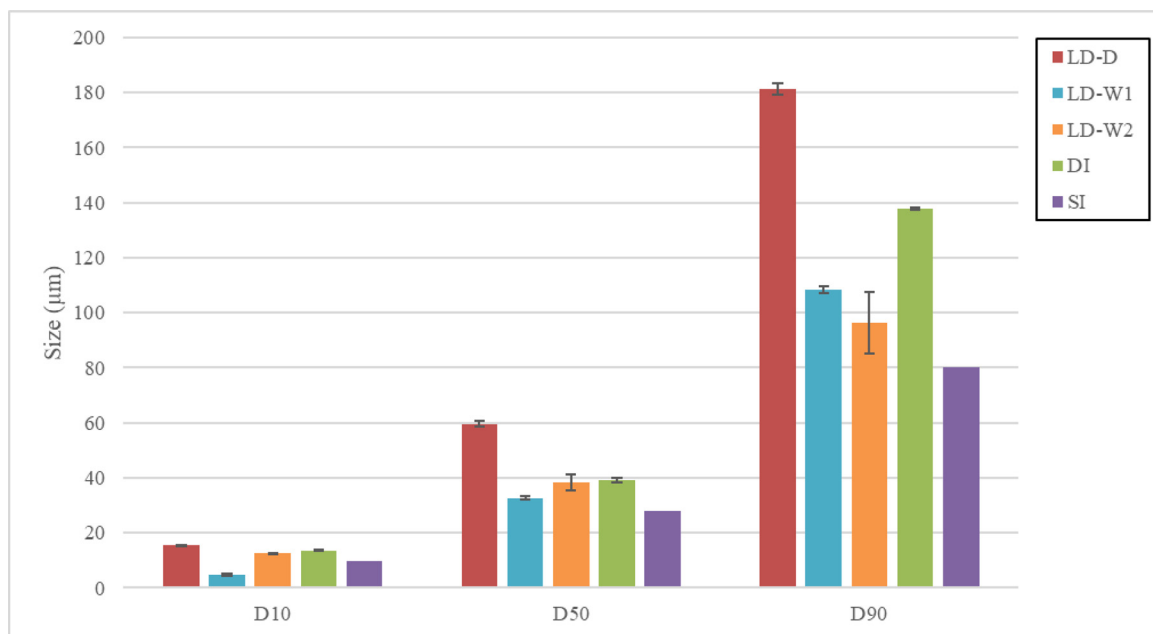


Fig. 8. PSD data for Powder 6, HIP.

There are five potential reasons for the differences seen in the sphericity and aspect ratio when comparing the DI and SI systems, which are:

- 1 Sample Quantity.** The sample quantity used for measurement purposes in the SI is significantly less compared to the DI (Table 1). The number of particles measured in the DI can be up to 1000 times more (dependent on the PSD) in comparison to the SI. The quality of the images from the SI is greater than the DI, however, the DI offers significantly higher sampling statistics;
- 2 Sample Orientation.** For the SI system, the sample is spread on a glass slide and images are taken. The sample will pick the orientation which is most stable in terms of positioning on the slide. For a perfectly spherical particle, the orientation will not influence the

result. Whereas a particle of irregular morphology (e.g. needle-like shape) will be strongly influenced by orientation, and the morphology characteristic can be exaggerated/missed. This is different from the DI system which takes images as the particles pass by a camera screen. The particle orientation will be random (as sometimes particles will align because of the airflow while falling) and not the same as that seen in the SI system, and therefore, certain characteristics maybe are neglected or overstated based on orientation during measurement for non-spherical particles;

- 3 Sample Preparation.** The SI system involves dispersing the sample by applying a burst of air pressure. This may knock off some of the loosely attached satellites/agglomerate, which therefore will influence the sphericity/aspect ratio value during measurement. The DI system involves a vibrator feed along with an air jet to disperse the

Table 6

Mean powder sphericity and aspect ratio measured via dynamic imaging and static imaging (volume basis).

	Sphericity		Aspect Ratio	
	DI	SI	DI	SI
Powder 1	0.90	0.97	0.90	0.94
Powder 2	0.91	0.92	0.87	0.88
Powder 3	0.90	0.94	0.88	0.91
Powder 4	0.92	0.96	0.90	0.93
Powder 5	0.91	0.97	0.86	0.94
Powder 6	0.90	0.96	0.85	0.93

sample. The air-jet does have the potential to break up some of the loose satellites/agglomerates;

4 Optics Resolution. The SI system is essentially a microscope, using objectives to take images of the stationary sample on a glass slide. The DI system is a CCD camera-based system taking images of powder as it moves past the field of view. The SI images have a higher resolution (sharper images of the boundary) in comparison to the DI, however, the number of particles imaged for SI is significantly lower in comparison to DI;

5 Edge Detection/Thresholding. Thresholding refers to the colour settings in determining the edge of the particles in the image analysis systems. This is generally determined by the manufacturer (factory set) though there is the possibility for the Raw data to be extracted and manually analysed by the operator. Typically, with the high magnification image, the particle edges are poorly resolved. The thresholding is important to determine the boundary between the background colour and the edge of the particle. Slight changes to this can impact the calculated particle size.

Steps were taken to minimise/remove the influences of the above-mentioned points by for example ensuring the dispersion pressure was set to a value to sufficiently spread the powder but not excessively high, however, it is possible that a combination of the mentioned reasons for varying magnitudes contributed to some of the differences in the data.

4. Conclusion

Six different metallic powders used in a range of applications (MIM, L-PBF, EB-PBF and HIP) were characterised in terms of PSD (D_{10} , D_{50} and D_{90}) using a range of laser diffraction and optical imaging techniques. Each powder was tested using laser diffraction systems (dry and wet) and imaging systems (dynamic and static). Samples that contained predominantly spherical powder produced fewer varying results over the range of equipment used to measure the PSD but still, enough variation existed to be problematic for tight tolerances common in critical applications (production of net shape components). Larger differences arose between the various measuring techniques, as the morphology of the sample deviated away from spherical, due to the presence of satellites either adhered to or fused onto larger particles, irregular particles and agglomerates. The differences seen in the measured PSD values were due to the contribution of assumed morphology during measurement. For a spherical particle the orientation is not critical during measurement as, regardless of the orientation for the measurement, it will measure the same in terms of PSD and not influence the result. However, for irregular or satellited particles, the influence of orientation becomes significant as the presence of these may be magnified or missed dependent on how the particle is positioned during the measurement. For example, if the satellites are positioned at the back or front of the sample during measurement via imaging, they may be missed, which has the potential to underestimate the PSD. Conversely, if the satellites are oriented on the side during measurement via laser diffraction, they have the potential to overestimate the PSD.

Furthermore, HIP powders proved challenging for the dry laser diffraction system, as the PSD was drastically overestimated due to agglomerates. This was not the case when using the wet laser diffraction system as the agglomerates were broken up during the suspension and circulation of the sample (future work outside the scope of this paper will be conducted to look at the measurement of PSD overtime in a wet cell to see how agglomerates are affected by the impeller). The static imaging system drastically under-measured the PSD for certain samples (HIP powders), and this was believed to be due to the sample dispersion which may not have been proportionally dispersed fine and coarse particles in samples with wide PSDs. Furthermore, the sample quantity measured also had the potential to bias the results, as for the static imaging technique, if a few large particles were missed during sampling, in addition to the sample quantity required for measurement being low (in comparison to the other measurement techniques), it could drastically underestimate the PSD.

Due to the discrepancies outlined, the following recommendations are offered

- Specifications for morphology (sphericity or aspect ratio) should always include a test method until discrepancies between DI and SI are better understood;
- Specifications and test methods should be aligned with production controls. Typically sieve analysis for 45 μm and above and laser diffraction below 45 μm ;
- If alternate test methods are to be used the bias between production control measurement and desired test method should be established and understood.

Declaration of Competing Interest

The authors declare that they have no known competing financial interests or personal relationships that could have appeared to influence the work reported in this paper.

Acknowledgements

The authors would like to thank Harry Oxley and Holger Krain (AMRC) for providing SEM images for the powders.

References

- [1] D.F. Heaney, R. Zauner, C. Binet, K. Cowan, J. Piemme, Variability of powder characteristics and their effect on dimensional variability of powder injection moulded components, *Powder Metall.* 47 (2) (2004) 144–149.
- [2] J. J. Dunkley, *Advances in atomisation techniques for the formation of metal powders*. Woodhead Publishing, 2013.
- [3] A. Mostafaei, C. Hilla, E.L. Stevens, P. Nandwana, A.M. Elliott, M. Chmiel, Comparison of characterization methods for differently atomized nickel-based alloy 625 powders, *Powder Technol.* 333 (Jun. 2018) 180–192.
- [4] Z. Snow, R. Martukanitz, S. Joshi, On the development of powder spreadability metrics and feedstock requirements for powder bed fusion additive manufacturing, *Addit. Manuf.* 28 (2019) 78–86.
- [5] P. Quinn, S. O'Halloran, J. Lawlor, R. Raghavendra, The effect of metal EOS 316L stainless steel additive manufacturing powder recycling on part characteristics and powder reusability, *Adv. Mater. Process. Technol.* 5 (2) (2019) 348–359.
- [6] O.A. Quintana, J. Alvarez, R. Mcmillan, W. Tong, C. Tomonto, Effects of reusing Ti-6Al-4V powder in a selective laser melting additive system operated in an industrial setting, *JOM* 70 (9) (Sep. 2018) 1863–1869.
- [7] Q.B. Nguyen, M.L.S. Nai, Z. Zhu, C.-N. Sun, J. Wei, W. Zhou, Characteristics of inconel powders for powder-bed additive manufacturing, *Engineering* 3 (5) (Oct. 2017) 695–700.
- [8] M. Ahmed Obeidi, et al., Comprehensive assessment of spatter material generated during selective laser melting of stainless steel, *Mater. Today Commun.* 25 (2020) 101294.
- [9] L. Cordova, M. Campos, T. Tinga, Revealing the effects of powder reuse for selective laser melting by powder characterization, *JOM* 71 (3) (Mar. 2019) 1062–1072.
- [10] A. Mussatto, R. Groarke, A. O'Neill, M.A. Obeidi, Y. Delaure, D. Brabazon, Influences of powder morphology and spreading parameters on the powder bed topography uniformity in powder bed fusion metal additive manufacturing, *Addit. Manuf.* 38 (2021) 101807.

- [11] A.T. Sutton, C.S. Kriewall, M.C. Leu, J.W. Newkirk, Powder characterisation techniques and effects of powder characteristics on part properties in powder-bed fusion processes, *Virtual Phys. Prototyp.* 12 (1) (2017) 3–29.
- [12] A. Califice, F. Michel, G. Dislaire, E. Pirard, Influence of particle shape on size distribution measurements by 3D and 2D image analyses and laser diffraction, *Powder Technol.* 237 (Mar. 2013) 67–75.
- [13] Y. Sun, M. Aindow, R.J. Hebert, Comparison of virgin Ti-6Al-4V powders for additive manufacturing, *Addit. Manuf.* 21 (2018) 544–555.
- [14] J.A. Slotwinski, E.J. Garboczi, P. Stutzman, C.F. Ferraris, S. Watson, M. Peltz, Characterization of Metal Powders Used for Additive Manufacturing, *J. Res. Natl. Inst. Stand. Technol.* 119 (Sep. 2014) 460–493.
- [15] R.J. Hebert, Y. Sun, M. Aindow, E.J. Garboczi, Three-dimensional particle size, shape, and internal porosity characterization: application to five similar titanium alloy (Ti-6Al-4V) powders and comparison to two-dimensional measurements, *Addit. Manuf.* 44 (2021) 102060.
- [16] H. G. Merkus, *Particle size measurements: fundamentals, practice, quality.* Springer Netherlands, 2009.
- [17] R. Groarke, R.K. Vijayaraghavan, D. Powell, A. Rennie, D. Brabazon, 18 - Powder characterization methods, standards, and state of the art, in: I. Yadroitsev, I. Yadroitseva, A. du Plessis (Eds.), *Additive Manufacturing Materials and Technologies*, Elsevier, 2021, pp. 491–527. E. B. T.F. of L. P. B. F. of M. MacDonald.
- [18] J. Grubbs, et al., Comparison of laser diffraction and image analysis techniques for particle size-shape characterization in additive manufacturing applications, *Powder Technol.* 391 (2021) 20–33.
- [19] J.G. Whiting, E.J. Garboczi, V.N. Tondare, J.H.J. Scott, M.A. Donmez, S.P. Moylan, A comparison of particle size distribution and morphology data acquired using lab-based and commercially available techniques: Application to stainless steel powder, *Powder Technol.* 396 (2022) 648–662.
- [20] L. Achelis, Characterisation of metal powders generated by a pressure-gas-atomiser, *Mater. Sci. Eng. A* 477 (1–2) (Mar. 2008) 15–20.
- [21] H. Mühlenweg, E.D. Hirleman, Laser diffraction spectroscopy: influence of particle shape and a shape adaptation technique, *Part. Part. Syst. Charact.* 15 (4) (Aug. 1998) 163–169.